Contents list available at IJRED website

International Journal of Renewable Energy Development

Journal homepage: https://ijred.undip.ac.id

Research Article

An investigation of the Steady-State and Fatigue Problems of a Small Wind Turbine Blade Based on the Interactive Design Approach

Khalil Deghoum[1,2], Mohammed T. Gherbi[2], Muhsin J. Jweeg[3], Hakim S. Sultan[4], Azher M. Abed[5], Oday I. Abdullah[6,7,8*], Necib Djilani[2]

[1]*UDERZA Laboratory, University of El Oued, 39000 El Oued, Algeria*

[2]*Department of Mechanical Engineering, University of El Oued, 39000 El Oued, Algeria*

[3]*College of Technical Engineering, Al-Farahidi University, Baghdad 10005, Iraq*

[4]*University of Warith Al-Anbiyaa, College of Engineering Karbala, Iraq*

[5]*Air Conditioning and Refrigeration Techniques Engineering Department, Al-Mustaqbal University College, Iraq*

[6]*Department of Energy Engineering, University of Baghdad, Iraq*

[7]*Department of Mechanics Al-Farabi Kazakh National University, Kazakhstan, Baghdad, Iraq*

[8]*System Technologies and Engineering Design Methodology, Hamburg University of Technology, Hamburg, Germany*

Abstract. A wind turbine blade is an essential system of wind energy production. During the operation of the blade, it is subjected to loads resulting from the impact of the wind on the surface of the blade. This leads to appear large deflections and high fatigue stresses in the structure of blades. In this paper, a 5 kW horizontal axis wind turbine blade model is designed and optimized using a new MATLAB code based on blade element momentum (BEM) theory. The aerodynamic shape of the blade has been improved compared with the initial design, the wind turbine power has been increased by 7% and the power coefficient has been increased by 8%. The finite Element Method was used to calculate the loads applied to the blade based on Computational Fluid Dynamics (CFD) and BEM theory. High agreements were obtained between the results of both approaches (CFD and BEM). The ANSYS software was also used to simulate and optimize the structure of the blade by applying variable static loads 3.3, 6, and 8.3 kg and compared the results with the experimental results. It was reduced the maximum deflections with 37%, 42.85%, and 42.61% when using CFRP material and 4.5%, 15.45%, and 16.19% for GFRP material that corresponds to the applied forces. Based on the results, the mass of the optimized model decreased by 47.86% for GFRP and 71.24% for CFRP. IEC 61400.2 standard was used to estimate the fatigue loads, damage, blade life prediction, and verify blade safety using a Simplified Load Model (SLM) and FAST software. It was found that the blade will be safe under extreme wind loads, and the lifetime of the wind blade (GFRP) is 5.5 years and 10.25 years, according to SLM and FAST software, respectively. At the same time, the lifetime of the wind blade (CFRP) is more than 20 years, according to the two applied methods.

Keywords: damage, composite materials, fatigue life, standard IEC 61400.2, Simplified Load Model, FAST software.

Received: 29th August 2022; Revised: 12th Nov 2022; Accepted: 8th Dec 2022; Available online: 18th Dec 2022

1. Introduction

Wind turbine energy is one of the most important sources used in the renewable energy sector. It is a source available everywhere in the world, where it is clean and free accessible. Wind turbines are used to generate electricity to supply homes, farms, factories, etc. (Rosato 2018).

The blade is the most important component of a wind turbine because it is responsible for rotating the generator to obtain electrical power. The process of optimizing the blade is an essential point from two different perspectives, the first one is to improve the external shape or aerodynamic characteristics to enhance the efficiency of the wind turbine. While the second one aims to improve the strength of the blade's structure so that it is more resistant to the loads applied on the surface of the blade due to wind and gravitational forces (Song *et al.* 2011).

Many recent studies used computational fluid dynamics (CFD) (Make *et al.* 2015) and the blade element momentum theory (BEM) (Tenguria *et al.* 2010) to calculate the aerodynamic loads. Also, to improve the aerodynamic characteristics and wind turbine power. Uchida *et al.* (2020) created a new approach for studying wind turbine farms based on computational fluid dynamics and a porous disk approach, and they explained the effect of vortices on the 2 MW wind turbines at various wind speeds. Zidane *et al.* (2020) simulated wind turbines in arid regions under the influence of sandstorms and debris flow based on the CFD and BEM methods and then coupled them with the neural network to study and improve the wind turbine performance. Ajirlo *et al.* (2021) simulated a micro wind turbine using CFD and BEM and compared it with the experimental results to develop a new model and verify the effect of the yaw angle on the extracted power.

* Corresponding author
Email: oday.abdullah@tuhh.de (OI Abdullah)

https://doi.org/10.14710/ijred.2023.48616
ISSN: 2252-4940/© 2023.The Author(s). Published by CBIORE

Modern wind turbines are manufactured from composite materials; as most of the studies in this field, these studies seek to develop the structure of the wind turbine blade to withstand the applied loads. The finite element method (FEM) is one of the most widely used methods for analyzing and optimizing blade structure. Peeters *et al.* (2018) achieved the numerical analysis of a wind turbine with a length of 43 m under static loads to obtain the results of displacements and local strains and then compare between FE model based on solid and FE model based on shell. Wu *et al.* (2012) based on the finite element analysis, studies the distribution and orientation of the fiber using the composite material of wind turbines. Pourrajabian *et al.* 2016) optimized the blade of the small wind turbines by studying the aero-structural design. Kim *et al.* (2009) studied the efficiency of large wind turbines under the influence of rotational and aerodynamic loads. Kim *et al.* (2013) created a new finite element model using an anisotropic material to develop the fabrication of a wind turbine based on the aeroelastic nonlinear multibody code (HAWC2 program). They also simplified the wind turbine model to a rectangular beam to get the results with lower time due to the complex shape of the blade.

Fatigue is one of the problems that occur to the material of the wind turbine blade when working for some time under fluctuating operating loads. That is why fatigue is one of the most important problems, and because of this, most researchers focus on this problem in their studies. Du *et al.* (2020) did a comprehensive study that provided the last six modern methods of detecting damage to wind turbine blades. (Bazilevs et al. 2016) predicted the fatigue damage of the wind turbine blade Sandia CX-100 of the full size that is made by composite materials using the fluid-structure interaction (FSI), and in their results reported the number of cycles until failure and the area of the most damage. Lee *et al.* (2015) performed an experimental work to study the fatigue failure of a 3 MW and length 56 m wind turbine blade at the root. They also used a FE model to verify the obtained results and gave more explanations. Rubiella *et al.* (2018) published a state-of-the-art paper and showed a method for calculating the fatigue loads of composite materials of wind turbines. The results showed large differences in the results. Shokrieh *et al.* (2006) used the FE model to simulate and predict the fatigue failure of composite material of the entire blade model and extracted the critical zone where the crack begins. Dervilis *et al.* (2014) deduced damage to a 9 m CX-100 wind turbine blade using Artificial Neural Networks (ANNs) and vibration modes.

Fatigue load is one of the complex problems due to the difficulty of complex interaction among the different parameters such as aerodynamics parameters, material, and fluctuating wind turbine loads. Therefore, the technical team of the International Electrotechnical Commission (IEC) has been trying for several years to simplify these loads for small wind turbines; its latest report was published under the IEC 61400-2 sequence (Commission 2013). The IEC report presented three methods for studying the fatigue of small wind turbines (testing, aeroelastic, and the simplified load model (SLM)). The new in these three methods is the SLM method, which has been divided into several cases. Each case was studied a specific load applied on a small wind turbine, such as fatigue load "case A" and extreme wind loads "case H". SLM approach is characterized by ease of use. Based on this approach, the computation time was reduced, and the safety factor was high (Wood 2009).

The current study aims to optimize the structure and material of the wind turbine blade with a power of 5 kW by studying the deflections and deformations under the influence of fluctuating wind. This study also aims to analyze and simplify the fatigue loads to calculate the damage and the number of fatigue cycles to predict the life of the wind turbine blade.

2. Blade structure design and FE model

The external structure of the blade consists of four basic parts: the shell, the neck, and the root, in addition to the spar cap. The function of the shell lies in building the aerodynamic structure and distributing the wind force on the blade's surface. As for the neck, it connects the shell and the root parts, and its purpose is to withstand the torques resulting from loads and deflection. While the root is used to connect the blade with the hub using metal screws, and the spar cap function is to resist flapwise of the blade, usually is not used in micro wind turbine blades. Fig.1-a. shows the main parts of the wind turbine blade.

In this study, BEM theory was used to design the blade (Tenguria *et al.* 2010). The airfoil NACA 4412 was chosen to design the aerodynamic shape of the blade, which the National Advisory Committee for Aeronautics created (NACA). The ratio of lift coefficient (Cl) to drag coefficient (Cd) at the angle of attack $\alpha = 5.25$ is 129.

The BEM theory is used to evaluate the applied load to the wind turbine blade, and it is also used to calculate the parameters of the blade geometry (twist angle (θ), chord length (c), and angle of attack (α)).

Matlab software was used to develop a new special code that solves the BEM equations using the iterative approach methods to calculate the chord and twist angle. Fig.2-a and Fig.2-b shows the results of the design parameters. Table 1. shows the details of specifications for the design parameters of a small wind turbine used in the first step to start the design process.

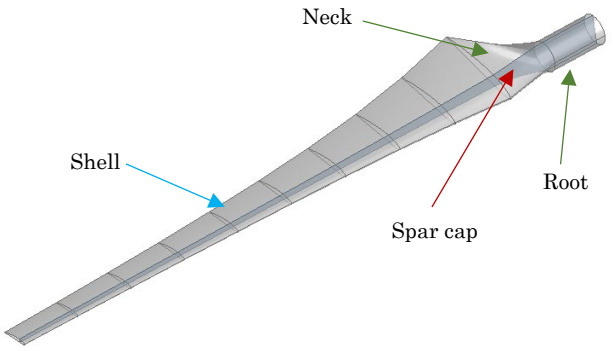

(a)

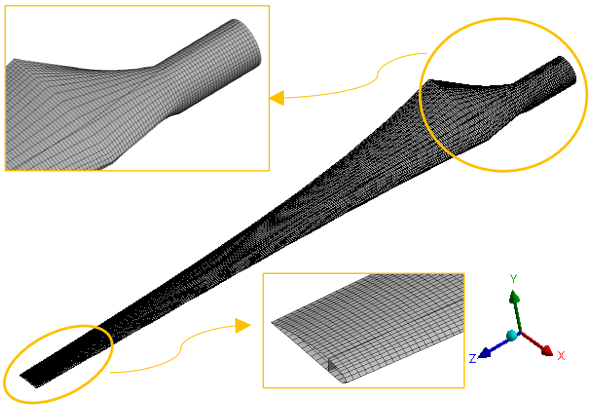

(b)

Fig.1 (a) part components of the blade and (b) FE model mesh

Table 1
The design parameters of a small wind turbine.

Design parameter	Value	Unit
Rated power	5	kW
Wind speed	10.5	m/s
Number of blades	3	-
Design tip speed ratio	6	-
Design angle of attack	5.25	°
Rotor radius	2.5	m
Design rotational speed	240	rpm
Density of air	1.22	kg/m3
Airfoil type	NACA4412	-

Table 2
Specifications design of 5 kW wind turbine blade.

Parameter	specification
root chord length	0.386 m
tip chord length	0.120 m
blade length	2.5 m
root diameter	0.080 m
hub length	0.300 m
hub to neck length	0.300 m

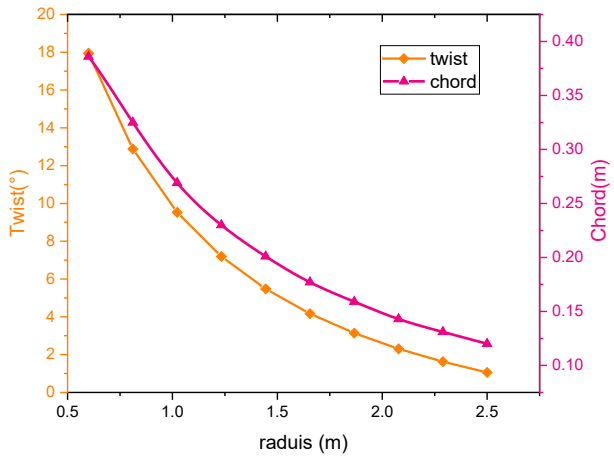

(a)

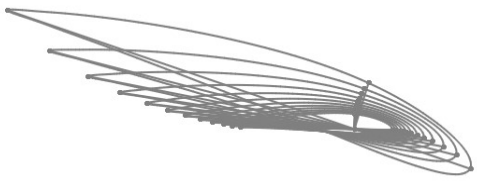

(b)

Fig.2 (a) Twist angle and Chord distribution, and (b) The twisted airfoil of 2.5 m small wind turbine blade

The commercial finite element method Ansys software was used to simulate the wind turbine blade model. For the blade mesh, the element "shell 281" was used, the element consists of eight-node Each node contains six degrees of freedom (DOF). mesh convergence is made depending on the error rate, which does not exceed 1 %. When the required convergence is reached, the number of nodes and the number of elements is determined. The last nodes of the FE model were 17820 elements and 18205 nodes. The final form of the FE mesh model is shown in Fig 1-b

Table 3
Mechanical properties of used material

Properties		GFRP	T300 CFRP
Young's modulus	E_{xx} (GPa)	44	136.7
	E_{yy} (GPa)	17	8.2
	E_{zz} (GPa)	16.7	8.2
Poisson's ratio	υ_{xy}	0.26	0.29
	υ_{zx}	0.26	0.42
	υ_{yz}	0.35	0.29
Shear modulus	G_{xy} (GPa)	3.49	4.45
	G_{zx} (GPa)	3.77	4.45
	G_{yz} (GPa)	3.46	2.91
Density	ρ (kg/m^3)	1800	1300

Source:(Korkiakoski *et al.* 2016), (Zhou *et al.* 2019)

3. Material properties of the blade

In this study, we will use composite materials to manufacture a wind turbine blade. In order to optimize the blade structure and reduce the deflection, we will choose the materials glass fiber reinforced polymer (GFRP) and carbon fiber reinforced polymer (CFRP), to create a FE model, and compare them with the experimental results to identify the most suitable material for manufacturing small wind turbine blades. the mechanical properties of the GFRP and CFRP materials are shown in Table 3.

To create the FE model of the blade made from composite materials, it needs to determine the direction of rotation of the fibers. This study selected the following sequence of the lay-up of the shell fibers: $[0/90]_3$ and $[0/90]_4$ for the CFRP and GFRP materials, respectively. At the same time, the lay-up sequence of the spar cap is $[45/-45]_3$. Each ply thickness is equal to 0.25 mm, with determines the direction of the length for the blade, i.e., the z-axis (see Fig. 1) is the 0° of the fiber lay-up sequence.

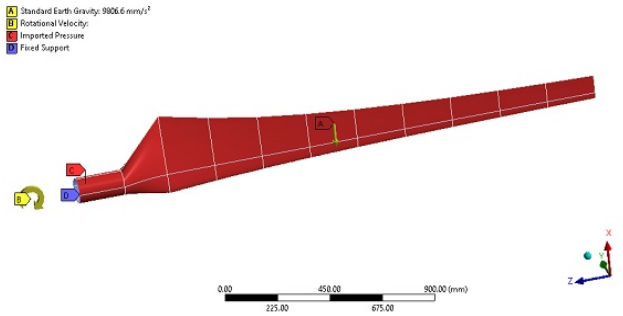

(a)

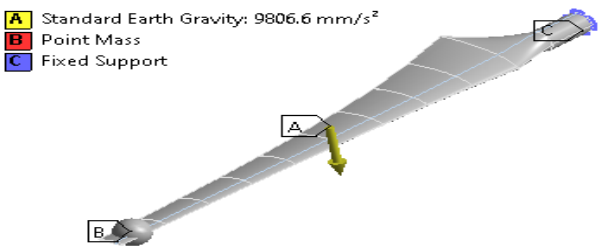

(b)

Fig.3 The boundary conditions of 2.5m wind turbine (a) load from CFD, and (b) static load

4. Blade boundary conditions

When the small wind turbine blade rotates, it will be subjected to pressure caused by wind speed in addition to the centrifugal force that results due to the rotation of the blade. The blade is fixed at the hub; therefore, all the DOF are null on the side of the root. Also, the force of gravity is affected by the blade's center of mass in a direction parallel to the tower. Fig. 3 shows the boundary conditions applied on the wind blade.

5. Study-state and aerodynamic load

To improve the structure of the wind turbine blade, it will discuss the comparison between the results of the FE model with the experimental results (Da Costa *et al.* 2020) and (Costa *et al.* 2017). In order to achieve this task, three magnitudes of static loads/ masses (3.3, 6, 8.3 kg) are fixed near the tip area to determine the maximum deflection of the blade tip.

During the operation of the wind blade, a collision occurs between the air stream that passes through the rotating wind turbine disk and the blade shell. These results appeared as aerodynamic loads (fluid-structure interaction-FSI). In order to calculate the aerodynamic loads, the computational fluid dynamics (CFD) method is adopted due to the possibility of simulating the 3D model by taking external influences such as blade tip vortices into consideration. Ansys Fluent software was used to simulate the wind turbine and compared the results with the BEM theory to verify the results. Fig.4 shows the aerodynamic loads applied to the blade surface section.

The fluent software uses the finite volume method (FVM) to solve the Navier-Stokes (N-S) equation (Bechmann et al. 2011). The main objective of solving this equation is to calculate the coefficients of normal force (Cn) and tangential force (Ct), in addition to the coefficient of drag force (Cd) and coefficient of lift force (Cl). The BEM theory and CFD simulation based on the equations 1 to 11 for obtaining the blade force and power results. It can be calculated the coefficient of lift and drag forces by Eq. 1 and Eq. 2 (Rosato 2018).

$$F_L = \frac{1}{2}\rho U_{rel}^2 c C_L \tag{1}$$

$$F_D = \frac{1}{2}\rho U_{rel}^2 c C_D \tag{2}$$

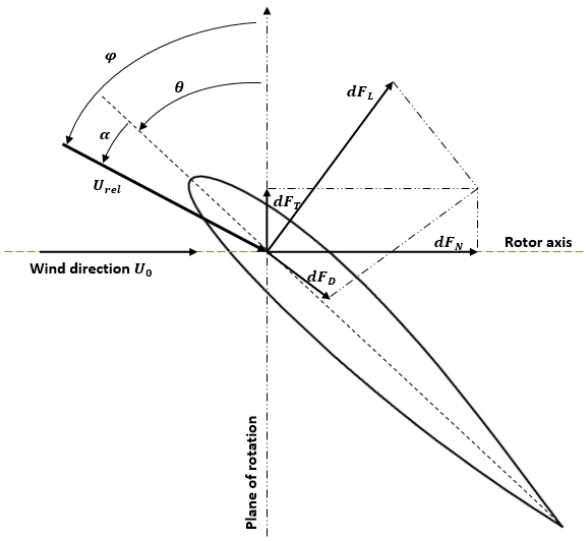

Fig 4. The airfoil section with aerodynamic loads and wind direction. α is the angle of attack and θ is the twist angle, φ is the inflow angle. FD, FL, FN, and FT are the drag force, lift force, normal force, and tangential force, respectively.

It can be calculated the normal coefficient force by using Eq.3 and Eq.4,

$$C_n = \frac{F_N}{\frac{1}{2}\rho U_{rel}^2 c} \tag{3}$$

$$C_n = C_L \cos\varphi + C_D \sin\varphi \tag{4}$$

It can be calculated the coefficient of the tangential force by Eq.5 and Eq.6

$$C_t = \frac{F_T}{\frac{1}{2}\rho U_{rel}^2 c} \tag{5}$$

$$C_t = C_L \sin\varphi - C_D \cos\varphi \tag{6}$$

It can be written the form of the relative wind velocity using Eq.7 (Liu *et al.* 2013),

$$U_{rel} = \sqrt{\left(\frac{\Omega R}{2}\right)^2 + (U_0)^2} \tag{7}$$

Where: c is the chord and $U_0$is the wind velocity.

In order to calculate the gravitational force and the centrifugal force, it can be using Eq. 8 and Eq. 9 (Rajadurai *et al.* 2008)

$$F_G = m_b g \tag{8}$$

$$F_C = m_b \omega^2 R \tag{9}$$

The rotor power is calculated from:

$$P = \mathrm{T}\omega \tag{10}$$

And the power coefficient are calculated from (Liu *et al.* 2013)

$$C_p = \frac{\mathrm{P}}{\frac{1}{2}\rho\pi R^2 U_0^2} \tag{11}$$

Where: F_G, and F_C are the gravitational and the centrifugal force, respectively. $m_b$is the blade mass, ω is the angular velocity of blade rotation, and T is the rotor torque

6. Aeroelastic simulation and SLM of IEC 61400-2

The wind turbine blade is exposed to fatigue due to the wind loads. In order to assess the impact of the loads on the blade of the wind turbine, an aeroelastic simulation should be created by developing a new model of a 5-kW wind turbine in the FAST software (version 7). This software is free and open-source software, it was developed by the National Renewable Energy Laboratory (NREL) (Jonkman *et al.* 2005). In order to start the simulation process using FAST software, the previous parameters of the blade (airfoil, blade length, rotation speed, etc.) will be used. The simplified load model (SLM) has also been adopted due to the straightforward with less complexity of model based on the primary loads with high safety factors (Wood 2009). The importance of SLM is to simplify the equations for calculating the forces acting on the root of the blade. SLM is divided into many parts that are arranged alphabetically (A to J), and each part is concerned with a specific case study.

6.1 SLM formulation (loads of case A)

Although all cases are in the SLM approach, the Normal operation is the only case that studies fatigue (Case A). The objective of SLM "case A" is to calculate the loads and predict the fatigue life of the blade and damage. The loads of case A based on SLM are applied to the root of the wind turbine blade. The flapwise moment of "case A" is applied in a range between the minimum value (50%) and the maximum value (150%). When applied the SLM equations, the generated stresses at the root are a combination of three forces: the centrifugal

force(ΔF_{zB}) in the direction of the blade tip, the flapwise moment (ΔM_{yB}) which is parallel to the blade length, and the lead-lag moment (ΔM_{xB}) in the direction of the rotation. The equations of case A are not included any unstable effects, such as the yaw error or the effect of gyroscopic loads. The following equations 12 to Eq 16 were used to calculate fatigue loads and compare the results with FAST simulation and the experimental work (Commission 2013; Evans *et al.* 2021; Evans 2017; Wood 2009):

$$\Delta F_{zB} = 2m_b r_g \omega_n^2 \quad (12)$$

$$\Delta M_{xB} = \frac{Q_{design}}{B} + 2m_b g r_g \quad (13)$$

$$\Delta M_{yB} = \frac{\lambda_{design} Q_{design}}{B} \quad (14)$$

$$Q_{design} = \frac{30 P_{design}}{\eta \pi \omega_n} \quad (15)$$

$$\eta = 0.6 + 0.005 P_{design} \quad (16)$$

Where: m_b is the mass of the blade, r_g is the radial distance from the center of the hub and the blade's center of gravity (0.880 m), and B is the number of blades. $\omega_n$is the design speed of rotation (rad/s), $P_{design}$is the design power, Q_{design} is the design torque (Nm), and η is the efficiency (limited between 0.6 and 0.7).

6.2. Equivalent stress and safety factors of the blade

In SLM approach, there is a difference in the equations for equivalent stresses σ_{eqB} according to the geometry of the root section (cylindrical or rectangular). In this study the fatigue was analyzed using the cylindrical shape of the root. In order to calculate the equivalent stresses of the case A, the following equation can be used (Wood 2009):

$$\sigma_{eqB} = \sigma_{zB} + \sigma_{MB} \quad (17)$$

Axial stress associated with centrifugal force is given by:

$$\sigma_{zB} = \frac{F_{zB}}{A_B} \quad (18)$$

Where A_B is the cross-section area of the blade root (5.024x10^{-3} m^2). The stress of bending σ_{MB} is given by:

$$\sigma_{MB} = \frac{\sqrt{M_{xB}^2 - M_{yB}^2}}{W_B} \quad (19)$$

Where: W_B is the section modulus of the blade (i.e., the second moment of inertia for the root section of the blade (m^4) divided by the distance between the root's centroid and the point of the maximum stress (m). For the current study, the blade section modulus is 5.5x10^{-5} m^3. It was found that the equivalent stresses of the fatigue load are σ_{eqB} =20.16 MPa.

SLM approach has a high safety factor and thus can be relied upon to calculate various stresses to verify the safety of the wind turbine blade. IEC standard 61400-2 has defined the partial safety factor based on the load type and the material's characterization. Where it was defined the safety factor for the loads (γ_f), as well as the safety factor for the materials (γ_m). Table 4 gives the partial safety factor values used in the IEC 61400-2. The material is assumed to be well characterized, so the partial safety factor for the minimum characterization is very high. This explains why most researchers used the full characterization (i.e., the lower safety factors). There are several conditions, including the blade properties derived from materials and configurations, representing the final structure. The fatigue tests were conducted with an acceptable load range and effects rate. Also, the material properties were calculated at a 95 % high probability and at a 95 % confidence level (Wood 2009).

The safety factors and the ultimate stress of SLM are used to determine the allowable stress σ_{all} according to the Eq. 20 (Wood 2009):

$$\sigma_{all} = \frac{\sigma_u}{\gamma_f \gamma_m} \quad (20)$$

Where: σ_u is the ultimate material strength. In other words, the final safety factor is obtained by multiplying the load safety factor γ_f and material safety factor γ_m. For the safety condition, the equivalent Von Mises stress must be less than the allowable stress:

$$\sigma_{eq} < \sigma_{all} \quad (21)$$

6.3 SLM (Loads of case H)

Small wind turbines often operate at wind speeds greater than the design wind speed. Owing this reason, the blade structure must be designed to withstand extreme wind loads. In the SLM approach, Case H is dedicated to the study of extreme wind loads applied to the blade. The objective of case H is to ascertain the rigidity of the blade structure and its resistance to extreme wind loads so that the blade is safe. In the case H equations, the design wind speed is not used to calculate the extreme wind loads, but the extreme wind speed for 50 years is used to calculate the flapwise moment and stresses. In the standard IEC 61400-2, wind turbines are categorized by average wind speed into Sections I to IV and Special Status S (Commission 2013). In this study, the design wind speed is 10.5 m/s, which means that the average wind speed is 7.5 m/s; this means that the section of the studied wind turbine is Class III according to IEC 61400-2, that is, the reference wind speed is U_{ref}= 37.5 m/s. Therefore, the extreme wind speed for 50 years can be determined by the equation $U_{e50} = 1.4\, U_{ref}$ =52.5 m/s. To calculate the equivalent stress σ_{MB} for case H it can be used the Eq. 23 (Commission 2013).

$$M_{yB} = \frac{1}{4} C_d \rho U_{e50}^2 A_{p,B} R = 1617.51 \text{Nm} \quad (22)$$

$$\sigma_{MB} = \frac{M_{yB}}{W_B} \quad (23)$$

WhereM_{yB}, is flapwise moment of the extreme wind speed and $A_{p,B}$ is the blade's projected area.

Table 4
Partial safety factors of IEC standard 61400-2 for loads and materials

Method	Partial safety factors for loads(γ_f)		Partial safety factor for the materials(γ_m)			
			Fatigue loads		Ultimate loads	
	Fatigue loads	Ultimate loads	Minimal characterization	Full characterization	Minimal characterization	Full characterization
SLM	1.0	3.0	10	1.25	3.0	1.1
aeroelastic	1.0	1.35	10	1.25	3.0	1.1

Source:(Commission 2013; Wood 2009)

6.4 Blade fatigue damage analysis

To assess the wind turbine blade damage caused by fatigue loads, it will apply the miner's law recommended by the standard IEC 61400-2. Miner's law relies on cumulative statistics to calculate the damage, and according to this law, the blade will fail if the damage exceeds a certain value. The following equation is used to calculate the damage of the blade: (Zhang *et al.* 2018)

$$D_B = \sum_i \frac{n_i}{N_f(\gamma_f \gamma_m \sigma_B)} \leq 1 \quad (24)$$

Where n_i is the number of performed cycles in bin i of the load characteristic spectrum, N_f is the number of cycles to failure, which is a variable function in terms of the stress level of fatigue cycles σ_B. The number of cycles to failure has a relationship to the associated stress level. For SLM, case A contains one 'bin' and it can be calculated the number of fatigue cycles by using Eq. 25,

$$n = \frac{B\Omega_{design} T_d}{60} = 7.59\text{x}10^9 \quad (25)$$

Where Ω_{design} is the rotational speed, T_d is the design life of the composite material of a wind turbine blade, where the lifetime is found to be about 20 years (i.e., $6.31\text{x}10^8$ s). In order to determine N_f, an S-N curve should be used; this curve will give the number of cycles to reach the failure versus maximum applied stress (stress level of fatigue cycles σ_B). At a constant stress ratio $\bar{R} = \sigma_{min}/\sigma_{max}$, the S-N curve of the composite material is a linear decreasing (i.e., the proportional relation between the stress and the $\log N_f$ is found). N_f can be calculated by applying the following Basquin's equation:(Hu et al. 2013),

$$\frac{\sigma_B}{\sigma_0} = 1 - \beta \log_{10} \mathrm{N_f} \quad (26)$$

Here σ_B is the maximum applied stress (associated stress level is 25.20MPa), σ_0 is the ultimate strength of the blade material, and β is the S-N curve slope coefficient of the materials.

7. Results and discussions

7.1 Power aerodynamic load of the blade

The aerodynamic structure of the blade has been improved to increase the power of the wind turbine. From Fig. 5-a, it can be noticed for the optimized design, the power coefficient increased when the tip speed ratio (TSR) is less than 4 and when TSR is greater than 6. This means that the range of increment for the power coefficient of the new improved design occurred within low and high periods of rotational speeds with an average increase of up to 8%. Fig. 5-b shows the power of the wind turbine for the initial and improved design, it can be observed that the power of the improved design increased when the wind speed is equal to or greater than 8 m/s. While the rated power at the rated wind speed is higher than by 7% compared with the initial design.

Fig. 6 shows the distribution of tangential and normal force coefficients. The CFD simulation and BEM theory were compared in seven different sections along the blade. As shown in Fig 6-a and Fig 6-b, the results are well approximated, and the difference between them is due to the difference in the calculation method because CFD studies a 3D model that depends on the number of elements and the number of nodes. At the same time, BEM method considers the blade as an ideal 1D rotating disk. The lift and the drag forces were calculated based on BEM method that was applied to the blade, and they were found to be 380.2 N and 7.9 N, respectively. At the same time, the gravitational force and the centrifugal forces were found to be 241.32 N and 1544.88 N, respectively.

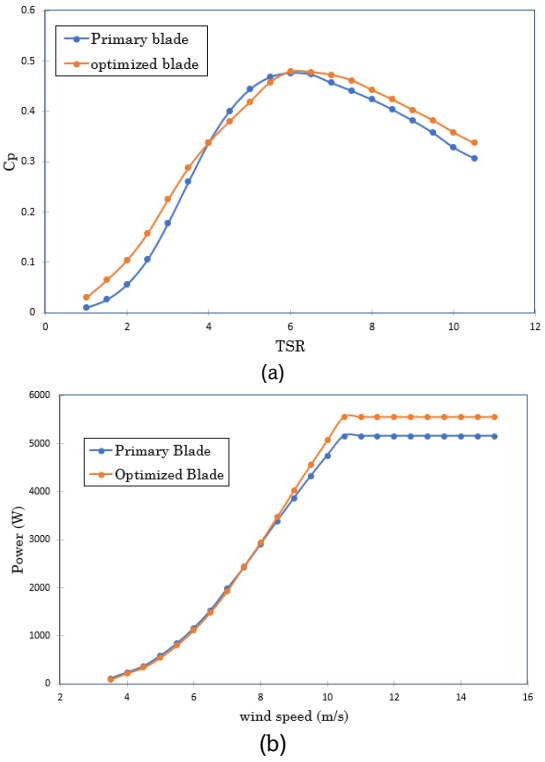

Fig. 5 (a) power coefficient, and (b) power for initial and optimized wind turbine blade rotor

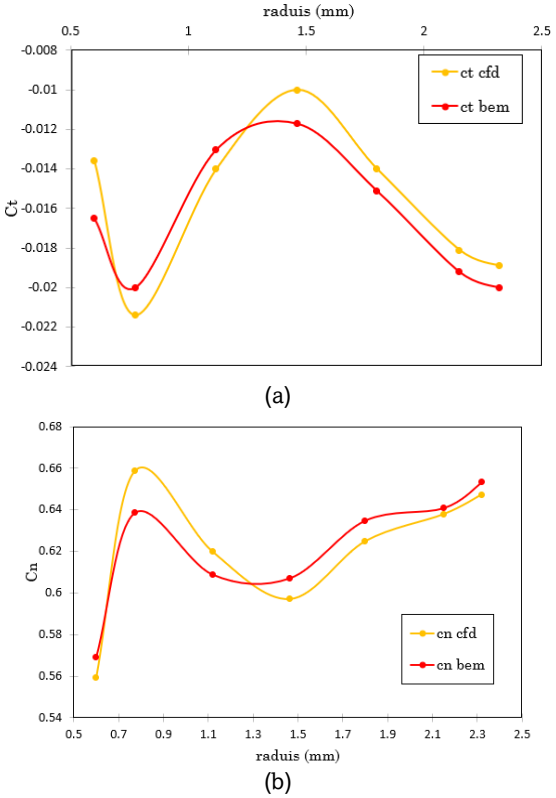

Fig.6 coefficient of **a**) tangential force and **b**) normal force

7.2 *Deflection of the blade under the static loads*

The wind turbine blade deflects due to the loads applied to the blade surface. The intensity of the loads varies with the wind speed. In the experimental study, (Costa et al. 2017; Da Costa et al. 2020) fabricated a wind turbine blade shell of GFRP and filled it with H80 foam with three loads/ masses (3.3, 6, and 8.3 kg) that were fixed near the blade tip to obtain the maximum blade deflection. In their study, the FE model was made from GFRP and CFRP to optimize the blade structure and the H80 foam change by the spar cap part to reduce the mass and study the deflection behavior of the blade.

Based on the obtained results, Fig.7 shows that the maximum deflections of the blade when applying a load of 3.3 kg for the CFRP and the GFRP materials are 23.08 mm and 35.35 mm, respectively. While the experimental deflection was 37 mm, its means that the deflections of carbon fiber and glass fiber are less by 37% and 4.5% compared to the experimental results. When applying a 6 kg load, the deflections of CFRP blade and GFRP blade are 40 mm and 59.18 mm, corresponding to 42.85% and 15.45% less than the experimental deflection (70 mm). When applying a load of 8.3 kg, the maximum deflection of the CFRP blade was 54.42 mm, which is 42.61% less than the experimental results, while the deflection of GFRP blade was 79.48 mm, which is 16.19% less than the experimental result (94.83 mm).

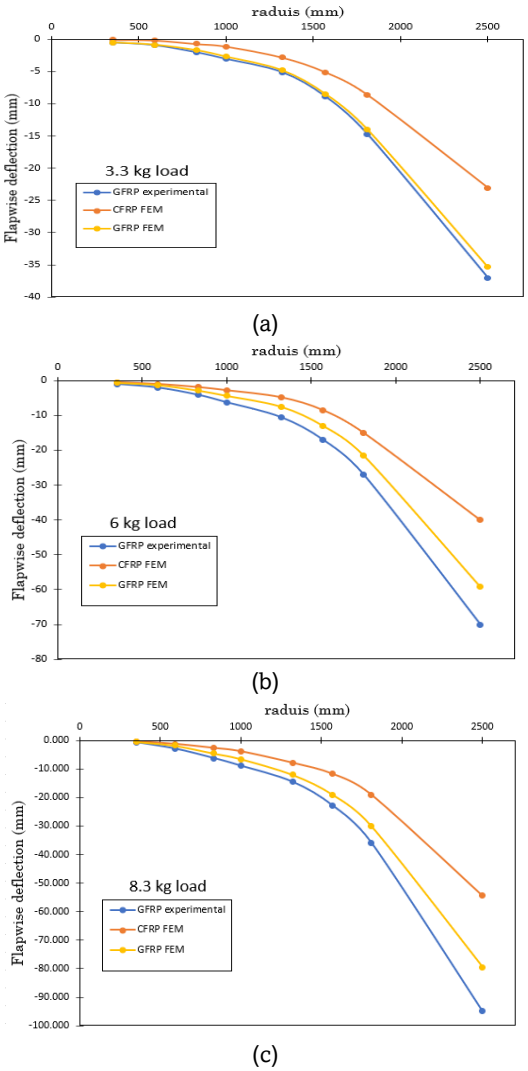

Fig.7 The blade flapwise deflection of a) 3.3 kg load and b) 6 kg load, and (c) 8.3 kg load.

When analysing the results, it can be noticed that the deflection of the blade made of CFRP material has the lowest deflection for all different loads. In contrast, the deflection of the blade of the GFRP material when carrying 3.3 kg was close to the experimental results. The difference in the deflection values increased when applying a load of 6 kg and 8.3 kg, which means that the improved structure of the blade appears due to resistance when applying significant loads. Despite the acceptable results of the enhanced structure of the blade in terms of deflection value, the enhanced value is evident in reducing the blade mass, as shown in Fig 8. Where the value of the blade mass in the experimental study is 6.3 kg, while the blade mass for the FE model of GFRP is 3.3 kg, which is reduced by 47.86%, The mass of the CFRP blade is 1.8 kg, which means the reduction is 71.24%.

7.3 Fatigue load calculation for SLM case A

Fig.9-a shows the flapwise moment of the wind turbine blade at 10.5 m/s design wind speed. Table 5 lists the fatigue loads under normal wind conditions. SLM approach considered the fatigue loads as a constant at a design speed. In fact, the blade will have a longer life due to the change in fatigue loads during periods of operation as well as periods of rest and maintenance. the SLM fatigue load changes with a constant sinusoidal field, and the maximum flapwise moment calculated by SLM is 1.5x ΔM_{yB}=952.38.

The results obtained by SLM approach were compared with the aeroelastic simulation of FAST software to validate the flapwise moment results. Fig.9-b shows the comparison between SLM and FAST approaches. It can be noticed that the flapwise moment of the SLM is constant over time. While it can be seen the fluctuation in the values when using the simulation of FAST software. The fluctuation in the values using FAST is due to the change in instantaneous wind speed and is closer to reality because the fatigue loads cannot always be constant.

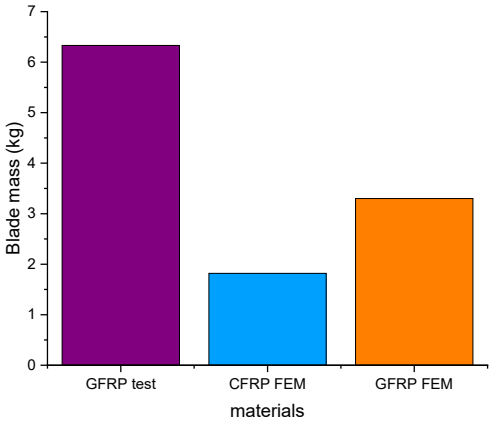

Fig.8 Mass of the wind turbine blade

Table 5
The fatigue Loads at normal wind conditions (10.5 m/s).

Loads type	SLM	FAST
Centrifugal force(kN)	27.49	23.83
Flapwise bending (Nm)	635	742
Edgewise bending (Nm)	531	1268
Design torque Q_{design}(Nm)	317	295

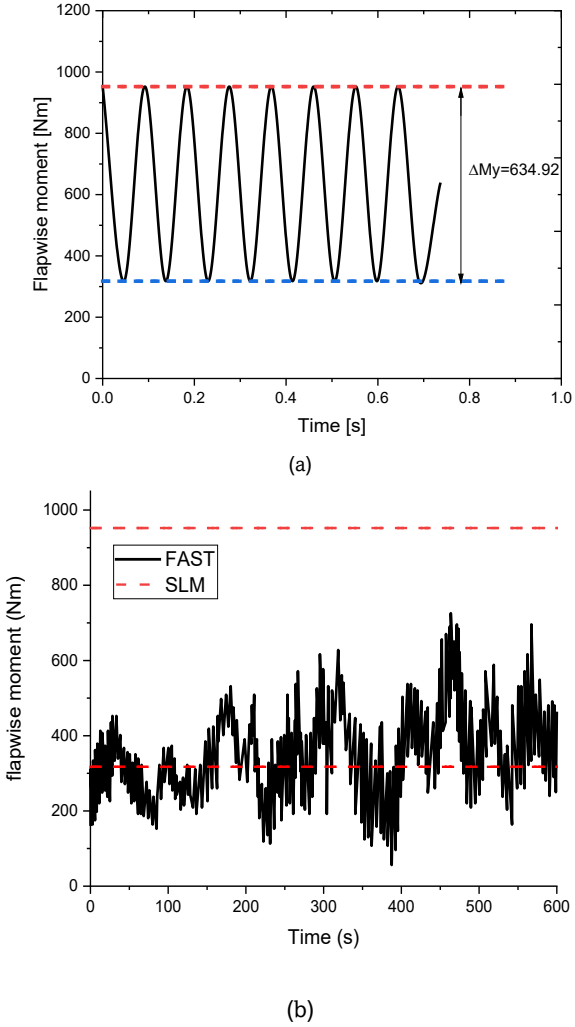

Fig.9 Flapwise moment of blade (a) the SLM sinusoidal range, and (b) comparison between SLM and fast simulation

7.4 Extreme wind load for SLM (case H)

In the case H of the SLM approach is imposed if the stress of the von Mises is less than the allowable stress limit, then the blade will be in a safe state. Table 6 shows the equivalent stress value of GFRP and CFRP blades which are 19.23 MPa and 26.84 MPa, respectively. Since the equivalent stress is less than the allowable stress limit, this means that the blade will be safe under extreme wind loads.

A simulation was performed using the ANSYS software to check the results of the SLM method. Initially, the CFD is used to study the effect of airflow at a wind speed of 52.5 m/s to calculate the pressure applied to the blade surface and then to the FE model to assess the stress at the root zone. Fig.10-a, b shows the distribution of von Mises stress on the blade for blades that are made from CFRP and GFRP materials.

From Fig. 10-a, b, it can be noticed that the average von-mises stress at the root of GFRP and CFRP blades are 20.58 MPa and 35.31 MPa, respectively, which means there is a convergence between the results of SLM and ANSYS in the distribution of von-mises stresses at the root zone. Hence, it can be concluded that the SLM "case H" results can be relied upon to verify the blade's safety when applying extreme wind loads.

Table 6
Extreme wind condition load case H of SLM

Material	Allowable Stress Limit (MPa)	Calculated equivalent Stress (MPa)	Conclusion
GFRP	151.52	19.23	SAFE
CFRP	248.48	26.84	SAFE

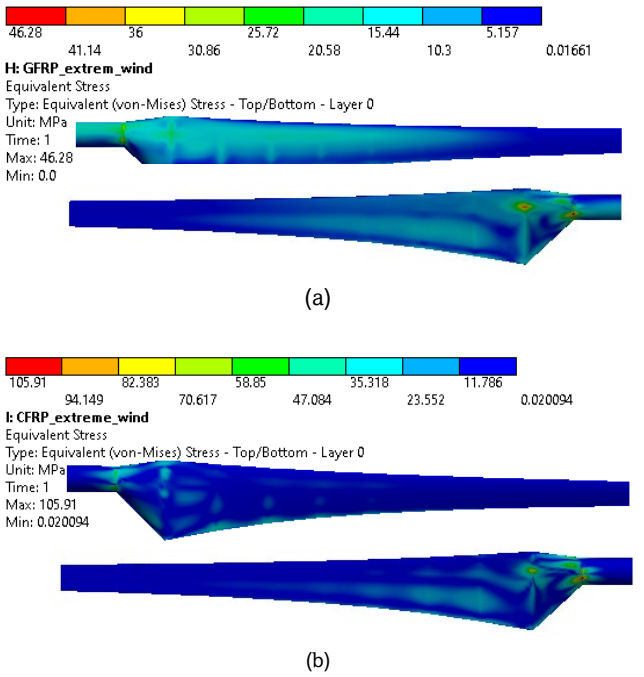

Fig.10 The von-Mises stress distribution of extreme wind conditions (a) GFRP material and (b) CFRP material

7.5 Damage analyses and blade life

In order to predict blade damage, Miner's law was applied. The GFRP material has an S-N slope parameter β of 0.106 (Mandell et al. 2002), and the CFRP material has a parameter less than 0.085 (Backe et al. 2018). Based on Eq.24, it was found that the number of cycles to reach the failure for the GFRP blade is $N_{f,GFRP} = 2.06\text{x}10^9$ cycles, and for the CFRP blade is $N_{f,CFRP} = 8.84 \times 10^{10}$. The damage of the GFRP blade was calculated by SLM approach and was found $D_{SLM,GFRP} = 3.68 > 1$. Since the damage is greater than 1, this means that the wind turbine blade will fail before reaching the design life. The damage of the blade (CFRP) is $D_{SLM,CFRP} = 8.59 \times 10^{-2}$, where the damage is less than one, this means that the blade will exceed the required design life. The damage was predicted by using M-Life of FAST software. The damage of the GFRP blade is found $D_{FAST,GFRP} = 2.01$, and for the CFRP blade it is found $D_{FAST,CFRP} = 4.27 \times 10^{-2}$.

According to SLM approach, a GFRP blade will withstand periodic fatigue loads for 5.5 years, while a CFRP blade will have a lifespan of more than 20 years. According to aerodynamic simulation achieved by FAST software, a GFRP blade will withstand loads for 10.25 years, while a CFRP blade will have a very long life of over 20 years. Table 7 compares the results obtained by SLM and FAST approaches with the experimental results of a wind turbine blade.

Table 7
Fatigue damage load and blade life for different methods and materials

Method	materials	SLM	FAST	Measured (Evans 2017)
Fatigue damage loads (Nm)		634	195	71
Blade fatigue life (years)	GFRP	5.5	10.25	9.18
	CFRP	over 20	over 20	-

From the previous results, it can be concluded that the SLM method is the most conservative (the safest results), followed by aeroelastic simulations, where the measured results are the least conservative. Somewhat disturbingly, all established methods predict a lifetime less than the design life of 20 years for the GFRP material, while the CFRP material has a fatigue life of more than 20 years.

8. Conclusions and future works

In this paper, the geometric parameters of the 5-kW blade are optimized using the MATLAB code developed based on the blade element momentum theory (BEMT). This paper aims to improve the blade structure and predict fatigue life.
As the first step in this study, the aerodynamic shape of the wind turbine blade was improved, and through the results, it was found that the power of the optimized shape increased by 7%, and the power coefficient increased by 8% compared to the initial design. Also, the aerodynamic loads using CFD and BEM were compared for the improved shape. Where, it was found that the results of both methods are compatible, and it can be relied upon them to find the aerodynamic loads. When applying different static mass/loads (3.3 kg, 6 kg, and 8.3 kg), the deflections of the GFRP blade were found to be 35.35 mm, 59.18 mm, and 79.48 mm, respectively.

At the same time, the deflections of the CFRP blade were found to be 23.08 mm, 40 mm, and 54.42 mm, respectively. On the other hand, the deflections of the optimized CFRP blade were reduced by (37%, 42.85%, and 42.61%) corresponding to the loads (3.3 kg, 6 kg, and 8.3 kg). While, it was found that the reductions of deflections for the optimized GFRP blade were (4.5%, 15.45%, and 16.19%) corresponding to the loads (3.3 kg, 6 kg, and 8.3 kg). The mass of the optimized blade structure was reduced by 47.86% when using GFRP and 71.24% when using CFRP, and it was also shown that the optimized blades made of CFRP and GFRP materials would be safe under extreme wind loads.

Furthermore, the blade damage was calculated using the SLM approach and FAST software. The percentage difference between the results of the two methods were 45.3% for GFRP and 50.29% for CFRP. The expected life of a wind turbine blade made of GFRP is 5.5 years, according to the SLM approach, and 10.25 years, according to the results of the FAST software. At the same time, the life of the blade made of CFRP material will be more than 20 years using both methods.

Assuming the gyroscopic loads play an essential role in the fatigue of wind turbine blades by affecting the root zone during blade yaw. Therefore, a developed approach in future research will be presented to predict the fatigue spectra of the small wind turbines caused by gyroscopic loads.

Funding: This research was funded by the University of Baghdad.

Conflicts of Interest: authors declare no conflict of interest.

References

Ajirlo, K. S., Tari, P. H., Gharali, K., & Zandi, M. (2021). Development of a wind turbine simulator to design and test micro HAWTs. *Sustainable Energy Technologies and Assessments*, 43100900; https://doi.org/10.1016/j.seta.2020.100900

Backe, S., & Balle, F. (2018). A novel short-time concept for fatigue life estimation of carbon (CFRP) and metal/carbon fiber reinforced polymer (MCFRP). *International Journal of Fatigue*, 116317-22 https://doi.org/10.1016/j.ijfatigue.2018.06.044

Bazilevs, Y., Korobenko, A., Deng, X., & Yan, J. (2016). Fluid–structure interaction modeling for fatigue-damage prediction in full-scale wind-turbine blades. *Journal of Applied Mechanics*, 83(6): https://doi.org/10.1115/1.4033080

Bechmann, A., Sørensen, N. N., & Zahle, F. (2011). CFD simulations of the MEXICO rotor. *wind energy*, 14(5): 677-89 https://doi.org/10.1002/we.450

Commission, I. E. (2013). IEC 61400-2: 2013-Wind Turbines. part 2. Small Wind Turbines. In. Australia: International Electrotechnical Commission

Costa, M. S., Evans, S. P., Bradney, D. R., & Clausen, P. D. (2017). A method to optimise the materials layout of small wind turbine blades. *Renewable Energy and Environmental Sustainability*, 219 https://doi.org/10.1051/rees/2017006

Da Costa, M., & Clausen, P. (2020). Structural Analysis of a small wind turbine blade subjected to gyroscopic load. In *Journal of Physics: Conference Series*, 042006. IOP Publishing https://doi:10.1088/1742-6596/1618/4/042006

Dervilis, N., Choi, M., Taylor, S., Barthorpe, R., Park, G., Farrar, C., & Worden, K. (2014). On damage diagnosis for a wind turbine blade using pattern recognition. *Journal of sound and vibration*, 333(6): 1833-50 https://doi.org/10.1016/j.jsv.2013.11.015

Du, Y., Zhou, S., Jing, X., Peng, Y., Wu, H., & Kwok, N. (2020). Damage detection techniques for wind turbine blades: A review. *Mechanical Systems and Signal Processing*, 141106445 https://doi.org/10.1016/j.ymssp.2019.106445

Evans, S., Dana, S., Clausen, P., & Wood, D. (2021). A simple method for modelling fatigue spectra of small wind turbine blades. *Wind Energy*, 24(6): 549-57 https://doi.org/10.1002/we.2588

Evans, S. P. (2017). Aeroelastic measurements, simulations, and fatigue predictions for small wind turbines operating in highly turbulent flow, The University of Newcastle, Australia; http://hdl.handle.net/1959.13/1349817

Hu, W., Park, D., & Choi, D. (2013). Structural optimization procedure of a composite wind turbine blade for reducing both material cost and blade weight. *Engineering Optimization*, 45(12): 1469-87 https://doi.org/10.1080/0305215X.2012.743533

Jonkman, J. M., & Buhl, M. L. (2005). *FAST user's guide* (National Renewable Energy Laboratory Golden, CO, USA).https://www.nrel.gov/wind/nwtc/fastv7.html

Kim, D.-M., Kim, D.-H., Park, K.-K., & Kim, Y.-S. (2009). Efficient Super-element Structural Vibration Analyses of a Large Wind-turbine Rotor Blade Considering Rotational and Aerodynamic Load Effects. *Transactions of the Korean Society for Noise Vibration Engineering*, 19(7): 651-58 https://doi.org/10.5050/KSNVN.2009.19.7.651

Kim, T., Hansen, A. M., & Branner, K. (2013). Development of an anisotropic beam finite element for composite wind turbine blades in multibody system. *Renewable Energy*, 59172-83, https://doi.org/10.1016/j.renene.2013.03.033

Korkiakoski, S., Brøndsted, P., Sarlin, E., & Saarela, O. (2016). Influence of specimen type and reinforcement on measured tension–tension fatigue life of unidirectional GFRP laminates. *International Journal of Fatigue*, 85114-29 https://doi.org/10.1016/j.ijfatigue.2015.12.008

Lee, H. G., Kang, M. G., & Park, J. (2015). Fatigue failure of a composite wind turbine blade at its root end. *Composite Structures*, 133878-85 https://doi.org/10.1016/j.compstruct.2015.08.010

Liu, X., Wang, L., & Tang, X. (2013). Optimized linearization of chord and twist angle profiles for fixed-pitch fixed-speed wind turbine blades. *Renewable Energy*, 57111-19 https://doi.org/10.1016/j.renene.2013.01.036

Make, M., & Vaz, G. (2015). Analyzing scaling effects on offshore wind turbines using CFD. *Renewable Energy*, 831326-40 https://doi.org/10.1016/j.renene.2015.05.048

Mandell, J. F., Samborsky, D. D., & Cairns, D. S. (2002). Fatigue of composite materials and substructures for wind turbine blades. In. Albuquerque, California: Sandia National Laboratories

Peeters, M., Santo, G., Degroote, J., & Van Paepegem, W. (2018). Comparison of shell and solid finite element models for the static certification tests of a 43 m wind turbine blade. *Energies*, 11(6): 1346 https://doi.org/10.3390/en11061346

Pourrajabian, A., Afshar, P. A. N., Ahmadizadeh, M., & Wood, D. (2016). Aero-structural design and optimization of a small wind turbine blade. *Renewable energy*, 87837-48 https://doi.org/10.1016/j.renene.2015.09.002

Rajadurai, J. S., Christopher, T., Thanigaiyarasu, G., & Rao, B. N. (2008). Finite element analysis with an improved failure criterion for composite wind turbine blades. *Forschung im Ingenieurwesen*, 72(4): 193-207 http://doi.org/10.1007/s10010-008-0078-8

Rosato, M. A. (2018). *Small Wind Turbines for Electricity and Irrigation: Design and Construction* (CRC Press: New York, USA)

Rubiella, C., Hessabi, C. A., & Fallah, A. S. (2018). State of the art in fatigue modelling of composite wind turbine blades. *International Journal of Fatigue*, 117230-45 https://doi.org/10.1016/j.ijfatigue.2018.07.031

Shokrieh, M. M., & Rafiee, R. (2006). Simulation of fatigue failure in a full composite wind turbine blade. *Composite Structures*, 74(3): 332-42 https://doi.org/10.1016/j.compstruct.2005.04.027

Song, F., Ni, Y., & Tan, Z. (2011). Optimization design, modeling and dynamic analysis for composite wind turbine blade. *Procedia Engineering*, 16369-75 https://doi.org/10.1016/j.proeng.2011.08.1097

Tenguria, N., Mittal, N., & Ahmed, S. (2010). Investigation of blade performance of horizontal axis wind turbine based on blade element momentum theory (BEMT) using NACA airfoils. *International Journal of Engineering, Science and Technology*, 2(12): 25-35 https://doi.org/10.1260/1708-5284.12.1.83

Uchida, T., Taniyama, Y., Fukatani, Y., Nakano, M., Bai, Z., Yoshida, T., & Inui, M. (2020). A new wind turbine CFD modeling method based on a porous disk approach for practical wind farm design. *Energies*, 13(12): 3197 https://doi.org/10.3390/en13123197

Wood, D. (2009). Using the IEC Simple Load Model for Small Wind Turbines. *Wind Engineering*, 33(2): 139-54 https://doi.org/10.1260/0309-524X.34.3.241

Wu, W. H., & Young, W. B. (2012). Structural analysis and design of the composite wind turbine blade. *Applied Composite Materials*, 19(3-4): 247-57 https://doi.org/10.1007/s10443-011-9193-z

Zhang, C., Chen, H.-P., & Huang, T.-L. (2018). Fatigue damage assessment of wind turbine composite blades using corrected blade element momentum theory. *Measurement*, 129102-11 https://doi.org/10.1016/j.measurement.2018.06.045

Zhou, S., & Wu, X. (2019). Fatigue life prediction of composite laminates by fatigue master curves. *Journal of Materials Research and Technology*, 8(6): 6094-105 https://doi.org/10.1016/j.jmrt.2019.10.003

Zidane, I. F., Swadener, G., Ma, X., Shehadeh, M. F., Salem, M. H., & Saqr, K. M. (2020). Performance of a wind turbine blade in sandstorms using a CFD-BEM based neural network. *Journal of Renewable and Sustainable Energy*, 12(5): 053310; https://doi.org/10.1063/5.0012272